

THERMAL DECOMPOSITION KINETICS OF RAW AND TREATED OLIVE WASTE

by

Zhihong WANG^{a,b}, Chengzhang WANG^{a,b*}, and Mijun PENG^c

^a Institute of Chemical Industry of Forest Products, Chinese Academy of Forestry, Nanjing, China

^b Key Laboratory of the Biomass Energy and Material, Nanjing, China

^c China National Analytical Center (Guangzhou), Guangzhou, China

Original scientific paper

<https://doi.org/10.2298/TSC171012078W>

The pyrolysis characteristic of raw and ultrasound assisted enzyme hydrolysis treated (UAEH) olive waste was investigated using the thermogravimetric analysis at 5, 10, 15, and 20 °C per minute in the nitrogen atmosphere. The thermal decomposition was divided into three stages in the thermograph curve, and the thermogravimetric curve showed the same decomposition trend for two samples. The temperature interval and peak temperature were different for two different samples, and moved to higher temperature with the increase in heating rate. Differential thermogravimetric and differential scanning calorimetry curves depicted that the structure and composition of samples were changed by UAEH. Meanwhile, the kinetic parameters were calculated by the Kissinger, Kissinger-Akahira-Sunose, Flynn-Wall-Ozawa, and Coats-Redfern methods. For untreated and treated olive waste, the Kissinger-Akahira-Sunose and Flynn-Wall-Ozawa methods revealed the similar kinetic characteristics for the conversion degree from 0.1 to 0.9, and the average values of activation energy were 201.42 kJ/mol and 162.97 kJ/mol, respectively. The change in activation energy was clearly dependent on the extent of conversion. The Coats-Redfern method suggested the second-order model (F_2 , $f(\alpha) = (1 - \alpha)^2$) could be used to better describe the thermal decomposition mechanism of untreated and treated olive waste. Besides, thermodynamic characteristics of olive waste treated were consistent with that of the untreated sample.

Key words: olive waste, pyrolysis, thermogravimetric analysis, kinetic, activation energy

Introduction

The traditional processing methods of biomass residues are becoming undesired owe to lands occupation, environment pollution and resource waste [1]. The results obtained from the previous study show that thermochemical conversion is a reasonable and efficient method to achieve the sustainable development [2-4]. At present, there are many common thermochemical conversion technologies, such as pyrolysis, gasification, and liquefaction [5]. Among these methods, pyrolysis is widely applied in thermal degradation process and effective for transforming biomass residues transformation into useful energy products [6]. The pyrolysis of biomass materials is considered carbon neutral process, because the amount of CO₂ released into the atmosphere during combustion is theoretically equivalent to the amount of photosynthesis absorbed during plant growth [7]. The knowledge of the kinetics of decomposition is a

* Corresponding author, e-mail: wangczl@sina.com, quliyifu@163.com

key factor in the evaluation of biomass materials, because thermochemical process depends on the operating conditions and the physical and chemical properties of the sample. The kinetic parameters, such as activation energy and pre-exponential factor, can be calculated for a constant extent of conversion by the iso-conversional methods [7, 8].

Generally, the degradation of biomass consists of four conversion step, including moisture dehydration, and then decomposition of hemicellulose, cellulose, and lignin. The thermal pyrolysis of biomass is a complex multiple process, mainly due to numerous and various thermochemical reaction [9, 10]. Olive waste which is the unique biomass residues has been widely concerned in olive production, energy, and waste disposal industries [11, 12]. Several studies dealing with the application of thermogravimetric (TG) analysis to evaluate pyrolysis behavior of olive residue were reported in the literature. Ounas *et al.* [13] used Flynn-Wall-Ozawa (FWO) and Vyazovkin methods to determine the apparent activation energy for the thermal decomposition of olive residues. The results showed that the activation energy of degradation of olive residues in the hemicellulose region was 153-162 kJ/mol, while that in the decomposition of cellulose region was 204-215 kJ/mol, and the differential thermogravimetric (DTG) plot suggested that olive residue mainly devolatilized around 473-673 K, with total volatile yield of about 70-75%. Ozveren *et al.* [14] investigated the slow pyrolysis profile of olive oil pomace through TG analysis coupled with mass spectrometry. The main mass loss occurred at 150-335 °C. The kinetics parameters were calculated by the ASTM E698, Friedman and Coats-Redfern (CR) methods. The activation energy were 170.99 kJ/mol, 173 kJ/mol, and 179.15 kJ/mol, respectively. From the previous results, the type of sample, treatment method and experimental model have a great influence on the pyrolysis characteristics and kinetic parameters. In addition, olive waste is considered a potential resource of phenolic that may be obtained as pivotal bioactive compounds [15]. Ultrasound-assisted enzymatic hydrolysis is one of the most efficient tools for extracting phenolic compounds from olive waste. The olive pomace with treated by ultrasound-assisted enzymatic hydrolysis exhibited a loose structure and rough appearance with the extensive presence of pores. Compared with the raw olive waste, the obvious changes of microstructure morphology were observed [16]. There are few reports on the pyrolysis characteristics of olive residues obtained after the extraction phenolic compounds by ultrasound-assisted enzymatic hydrolysis, and the olive stone is removed.

The objective of this work was to investigate the pyrolysis characteristics for untreated olive waste (removed stone) and treated through ultrasound-assisted enzymatic hydrolysis using TG analysis method at different heating rates under nitrogen atmosphere. The decomposition behaviors were compared by DTG and differential scanning calorimetry (DSC) curves. Furthermore, the kinetic parameters were calculated and pyrolysis mechanism was explained through iso-conversional Kissinger method, Kissinger-Akahira-Sunose (KAS) models, FWO models, and CR method. Meanwhile, the thermal decomposition thermodynamic characteristics of the untreated and treated olive waste were also identified.

Materials and methods

Materials

Olive waste was obtained from an olive oil production company, namely Xiangyu (Gansu, China) in October 2016, and stored at -20 °C until use. The experiments were performed by adding 500 g olive waste into a 2.0 L buffer solution. The mixture was then stirred. The precipitation of olive stone was removed from the system. A 50 g enzyme mixture was added to the rest of solid-solution mixture. The sample was treated during 30 minute at 50 °C

by the ultrasound-assisted enzyme hydrolysis and filtered. Then the filter residue was dried at 60 °C until constant weight and was stored for the further analysis.

The enzyme mixture was prepared using cellulose (20000 U/g, pH 4.8-5.2, temperature 55-60 °C), hemicellulose (10000 U/g, pH 4.0-5.5, temperature 30-60 °C) and pectinase (20000 U/g, pH 2.5-5.0, temperature 30-55 °C) from Sukahan Biological Engineering Co., Ltd (Shandong, China), and the ratio was 1:1:1. The buffer solution (pH 5.75) in the experiment was prepared according to different ratio of disodium hydrogen phosphate and citric acid.

Thermogravimetric analysis of the olive waste

The experiments were performed in a TG analyzer (NETZSCH TG-209 F1, Germany) under nitrogen atmosphere (purity of 99.99%, the flow rate of 20 mL per minute). In every experiment, approximately 5.0 mg of sample was put in the platinum TG analyzer crucible and heated from 35 to 900 °C with the heating rate of 5 °C per minute, 10 °C per minute, 15 °C per minute and 20 °C per minute. The TG and derivative thermogravimetric curves were observed by the TG analysis.

Differential scanning calorimetry analysis of the olive waste

Thermograms were obtained from DSC calorimeter (NETZSCH STA 409 PC/PG, Germany). The weight of the samples for DSC measurements was maintained at about 5.0 mg. The sample was heated at a constant rate of 10 °C per minute from 40 °C to 600 °C under nitrogen atmosphere with a nitrogen flow rate of 50 mL per minute. The DSC thermograms were obtained as a function of temperature and heat flow.

Kissinger method

Kissinger method [17, 18] is a model-free non-isothermal method. It is not necessary to calculate the activation energy of each conversion value in order to evaluate kinetic parameters using the method:

$$\ln\left(\frac{\beta}{T_{\max}^2}\right) = \ln\left(\frac{AR}{E_{\alpha}}\right) - \frac{E_{\alpha}}{RT_{\max}} \quad (1)$$

The plot of $\ln(\beta/T_{\max}^2)$ against $1/T_{\max}$ gives a straight line from which the slope gives the activation energy E_{α} .

The KAS method

The KAS models [18, 19] are one of the most widely used iso-conversional methods to evaluate pyrolysis kinetics, which is based on the equation:

$$\ln\left(\frac{\beta}{T^2}\right) = \ln\left(\frac{AE_{\alpha}}{Rg(\alpha)}\right) - \frac{E_{\alpha}}{RT} \quad (2)$$

The plot of $\ln(\beta/T^2)$ against $1/T$ gives a straight line from which the slope gives the activation energy E_{α} .

The FWO method

The FWO models [20, 21] are another most common and widely accepted methods to determine the kinetic parameter. The form of the FWO equation is expressed:

$$\ln \beta = \ln \left(\frac{AE_\alpha}{Rg(\alpha)} \right) - 5.331 - 1.052 \left(\frac{E_\alpha}{RT} \right) \quad (3)$$

The plot of $\ln \beta$ vs. $1/T$ gives a straight line with the slope gives the activation energy E_α , and the pre-exponential factor A can be calculated from the intercept.

The CR method

The CR model is derived from Arrhenius equation and can be used to calculate activation energy, pre-exponential factor and apparent reaction order [22]. The equation for numerical determination of the kinetic parameters using the CR method is given:

$$\ln \left[\frac{g(\alpha)}{T^2} \right] = \ln \left[\frac{AR}{\beta E_\alpha} \left(1 - \frac{2RT}{E_\alpha} \right) \right] - \frac{E_\alpha}{RT} \quad (4)$$

The slope of plot $\ln[g(\alpha)/T^2]$ against $1/T$ at different heating rates can be employed to determine the value of apparent activation energy E_α at a constant value of α , tab. 1.

Table 1. The most common reaction mechanism functions of CR method and their integral forms

Model	Reaction mechanism	$f(\alpha)$	$g(\alpha)$
Order-based	First-order (F_1)	$1 - \alpha$	$-\ln(1 - \alpha)$
	Second-order (F_2)	$(1 - \alpha)^2$	$(1 - \alpha)^{-1} - 1$
	Third-order (F_3)	$(1 - \alpha)^3$	$[(1 - \alpha)^{-2} - 1]/2$
Diffusional	1-D diffusion (D_1)	$1/2\alpha$	α^2
	2-D diffusion (D_2)	$[-\ln(1 - \alpha)]^{-1}$	$\alpha + (1 - \alpha)\ln(1 - \alpha)$
	3-D diffusion (D_3)	$[(3/2)(1 - \alpha)^{2/3}]/[1 - (1 - \alpha)^{1/3}]$	$[1 - (1 - \alpha)^{1/3}]^2$
	Ginstling-Brounshtein (D_4)	$[(3/2)(1 - \alpha)^{1/3}]/[1 - (1 - \alpha)^{1/3}]$	$(1 - 2\alpha/3) - (1 - \alpha)^{2/3}$
Nucleation	Avrami-Erofeev (A_2)	$2(1 - \alpha)[- \ln(1 - \alpha)]^{1/2}$	$[- \ln(1 - \alpha)]^{1/2}$
	Avrami-Erofeev (A_3)	$3(1 - \alpha)[- \ln(1 - \alpha)]^{1/3}$	$[- \ln(1 - \alpha)]^{1/3}$
Geometrical contraction	Contracting area (G_2)	$2(1 - \alpha)^{1/2}$	$[1 - (1 - \alpha)^{1/2}]$
	Contracting volume (G_3)	$3(1 - \alpha)^{1/3}$	$[1 - (1 - \alpha)^{1/3}]$
Power law	2/3-Power law (P_{23})	$(2/3)\alpha^{-1/2}$	$\alpha^{3/2}$

Due to the energy compensation effects, the variation between activation energy and pre-exponential factor must be considered [23, 24]. The equation was given:

$$\ln A = aE_\alpha + b \quad (5)$$

where a and b are constants and can be calculated from the slope and intercept of the fitting straight line of $\ln A$ vs. E_α .

Thermodynamic parameters calculation

Based on the previous experiment, enthalpies, ΔH , Gibbs free energies, ΔG , and entropies, ΔS , are be calculated from [4]:

$$A = \frac{\beta E_\alpha \exp \left(\frac{E_\alpha}{RT_m} \right)}{RT_m^2} \quad (6)$$

$$\Delta H = E_a - RT_{\max} \quad (7)$$

$$\Delta G = E_a + RT_{\max} \ln \left(\frac{K_B T_{\max}}{hA} \right) \quad (8)$$

$$\Delta S = \frac{\Delta H - \Delta G}{T_{\max}} \quad (9)$$

Results and discussion

Thermogravimetric analysis of olive waste

As shown in figs. 1 and 2, the thermograph indicated the evolution in weight loss and extent conversion of untreated and treated olive waste with the increasing temperature under the heating rate of 5, 10, 15, and 20 °C per minute.

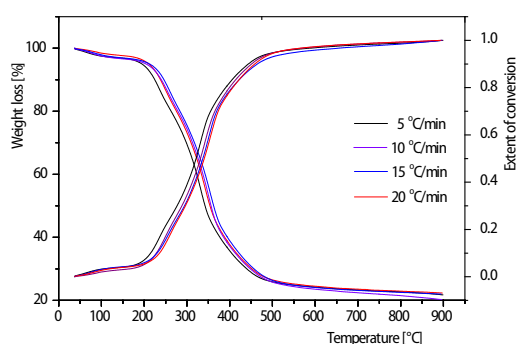


Figure 1. The TG and extent of conversion curves of raw olive waste

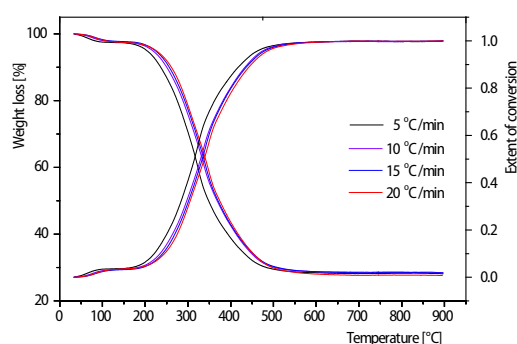


Figure 2. The TG and extent of conversion curves of treated olive waste

Table 2 showed the profile of weight loss of raw and treated olive waste at the different heating rates. The first stage mainly included the dehydration of moisture and release of light volatile matters [1]. Furthermore, volatile ingredients were degraded in this temperature range. The second stage, which may be caused by the decomposition of the hemicellulose, cellulose, and lignin at the temperature ranges, was crucial for the whole pyrolysis process [2]. Table 2 showed the second stage temperature interval of olive waste untreated were 137-485 °C for the

Table 2. Temperature intervals and weight loss of different regions for olive waste

Sample	Heating rate [°Cmin ⁻¹]	Temperature intervals [°C]			Weight loss of sample [%]		
		First	Second	Third	First	Second	Third
Raw olive waste	5	35-137	137-485	485-900	3.021	70.58	4.638
	10	35-144	144-505	505-900	2.279	71.42	3.966
	15	35-149	149-515	515-900	3.369	71.41	4.984
	20	35-152	152-530	530-900	3.112	71.64	3.257
Treated olive waste	5	35-132	132-483	483-900	2.605	67.38	1.951
	10	35-142	142-489	489-900	2.418	67.04	2.137
	15	35-148	148-504	504-900	2.299	67.51	1.802
	20	35-152	152-514	514-900	2.583	68.08	1.734

5 °C per minute heating rate, for the 10 °C per minute is 144-505 °C, for the 15 °C per minute is 149-515 °C and for the 20 °C per minute is 152-530 °C. In this zone, the weight losses were 70.58 wt.%, 71.42 wt.%, 71.41 wt.%, and 71.64 wt.% at the heating rate of 5, 10, 15, and 20 °C per minute respectively during the pyrolysis process. Simultaneously, the maximum weight loss and the temperature interval were observed from the tab. 2. In the third stage, the weight loss for two samples reached to constant weight at for the different heating rates with the increase of temperature. In the stage, the final decomposition involved the aromatization process of lignin fraction, resulting in a very low weight loss. Finally, the thermal stable groups of char prevented the further degradation [13]. Besides, figs. 1 and 2 also presented that the extent of conversion increase with increasing temperature at any heating rate, the literature from Islam *et al.* [4] reported the similar behavior for the pyrolysis of karanja fruit hulls char using TG analysis. Table 2 also presented that the main weight loss was observed in the second step, and the temperature intervals moved to the high temperature with increasing the heating rate.

The DTG curves displayed the similar trend at the four different heating rates for different samples, figs. 3 and 4. The relatively high and narrow peaks were observed in the second pyrolysis stage from the DTG profile at the given heating rate. The peak temperatures of untreated olive waste were 331.6 °C, 340.6 °C, 349.6 °C, and 353.3 °C, respectively. Furthermore, these temperatures were high compared to the peak temperature for the treated sample in the different heating rate. These peaks implied that the maximum rate of weight loss relied mainly on the hemicellulose, cellulose, and lignin after dehydration. Because the sample reached the designed temperature in a short time with the high heating rate, and the thermal lag was increased [13]. In addition, compared to the DTG curves of treated olive waste, an obvious shoulder in the temperature range of 230-260 °C was observed in each DTG patterns of heating rate. It was worth noting that weight loss might be caused by volatile components and bioactive substance in the temperature range. Therefore, the decomposition was affected by some pivotal factors, including structure composition, temperature, and heating rate by TGA.

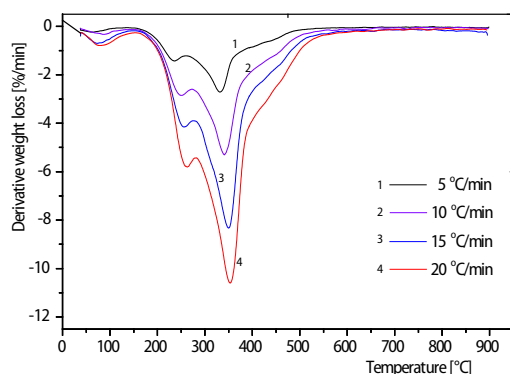


Figure 3. The DTG curve of raw olive waste

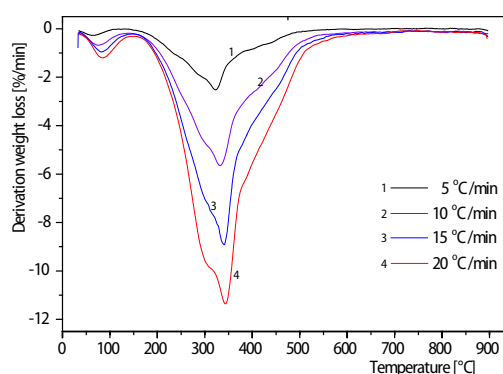


Figure 4. The DTG curve of treated olive waste

Differential scanning calorimetry analysis of olive waste

The DSC thermographs of raw and treated olive waste were presented in fig. 5. As shown in fig. 5, in the temperature range of 80-100 °C, the broad endothermic peaks were observed for both samples, which corresponded to the evaporation of absorbed water by olive waste [25]. Additionally, the DSC curves of the two samples were significantly different, compared to the olive waste treated, the DSC thermogram of olive waste showed two distinct en-

dothermic peaks, at 250 °C and 438 °C, respectively. And the broad endothermic peak observed around 250 °C indicated the degradation of valuable substances, which could be extracted by ultrasound assisted enzyme hydrolysis. The stronger endothermic peak at 438 °C might be closely related to the degradation of lignin. In the DSC curve of olive waste treated, the small endothermic peak obtained around 360 °C suggested the decomposition of cellulose, leading to char formation [25]. Therefore, the DSC curves illustrated that the heat flow required of olive waste treated by ultrasound assisted enzyme hydrolysis was significantly different from the untreated sample. It also showed that ultrasound assisted enzyme hydrolysis can be used to extract effectively the valuable substance and the structure of sample was changed by this technology.

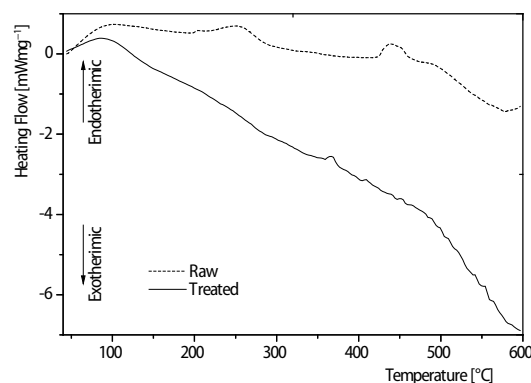


Figure 5. The DSC thermograph of raw and treated olive waste

Activation energy determined by Kissinger method

Based on the linear equation, the values of E_a and A from Kissinger method, were 183.57 kJ/mol, 180.78 kJ/mol, and $1.046 \times 10^{11} \text{ min}^{-1}$, $4.812 \times 10^6 \text{ min}^{-1}$ for untreated and treated olive waste samples, respectively. One set of kinetic parameters was calculated for a specified temperature from the Kissinger method [17].

Activation energy determined by KAS and FWO methods

The activation energy could be calculated according to slopes from the liner plot of $\ln(\beta/T^2)$ vs. $1/T$ and $\ln(\beta)$ vs. $1/T$. The extent of conversion was increased from 0.1 to 0.9, and the activation energy was calculated by the KAS and FWO methods, respectively. Subsequently, the activation energy calculated and corresponding correlation coefficient were presented in tab. 3. Meanwhile, the relative difference between the activation energies calculated with the KAS method and the ones obtained with FWO method was included in the analysis of the results. The analysis of results for untreated and treated olive waste revealed that the activation energy obtained from KAS and FWO methods at each decomposition stage were very similar and their variation with the conversion extent was also coincident.

For the untreated olive waste, when the extent of conversion was 0.8, the activation energy required was the maximum, which suggested the energy barrier of olive waste combustion was higher compared to that of another conversion degree. The activation energies in the 0.1-0.8 conversion range have a value of 128.37-301 kJ/mol and 129.90-297.26 kJ/mol for KAS and FWO methods, respectively. When the extent of conversion was 0.9, the activation energies have dropped to 221.90 kJ/mol and 222.46 kJ/mol. The activation energy averages were 202.06 kJ/mol and 200.77 kJ/mol for these two methods. For the treated olive waste, based on the KAS methods, when the extent of conversion value increased from 0.1 to 0.4, the activation energy gradually raises from 114.16 kJ/mol to 170.85 kJ/mol, and then the value basically kept steady within conversion range of 0.4-0.5, which attributed to the pyrolysis of hemicellulose and cellulose. With the process of pyrogenation, the activation energy values decreased smoothly from 170.37 kJ/mol to 153.89 kJ/mol when the extent of conversion value continued to increase from

Table 3. The parameters for different conversion value obtained by KAS and FWO models

Sample	Conversion value	KAS			FWO			Difference [%]
		E_a [KJmol ⁻¹]	A [min ⁻¹]	R^2	E_a [KJmol ⁻¹]	A [min ⁻¹]	R^2	
Raw olive waste	0.1	128.37	7.82E+3	0.9843	129.90	2.93E+12	0.9860	1.19
	0.2	139.92	3.36E+4	0.9909	141.32	1.39E+13	0.9882	1.00
	0.3	159.72	5.33E+5	0.9928	153.16	4.79E+13	0.9992	4.11
	0.4	197.94	3.81E+8	0.9951	197.39	1.99E+17	0.9964	0.28
	0.5	204.18	5.00E+8	0.9959	203.63	2.79E+17	0.9963	0.27
	0.6	214.91	2.00E+9	0.9960	214.06	1.17E+18	0.9963	0.39
	0.7	250.02	5.82E+11	0.9937	247.73	3.64E+20	0.9942	0.92
	0.8	301.55	6.81E+14	0.9944	297.26	4.76E+23	0.9948	1.42
	0.9	221.90	5.28E+7	0.9821	222.46	4.27E+16	0.9750	0.25
Average	202.06			200.77				
Treated olive waste	0.1	114.16	184.42	0.9987	116.51	7.06E+10	0.9965	2.06
	0.2	129.74	1.86E+3	0.9977	131.86	8.14E+11	0.9998	1.63
	0.3	157.95	3.05E+5	0.9977	159.03	1.46E+14	0.9934	0.68
	0.4	170.86	1.94E+6	0.9940	171.61	9.96E+14	0.9978	0.44
	0.5	170.37	8.94E+5	0.9997	171.42	4.87E+14	0.9989	0.62
	0.6	165.71	2.27E+5	0.9980	167.23	1.29E+14	0.9999	0.92
	0.7	153.89	1.27E+4	0.9991	156.33	7.67E+12	0.9955	1.59
	0.8	171.55	1.14E+5	0.9992	173.59	7.63E+13	0.9960	1.19
	0.9	225.80	2.76E+8	0.9971	225.83	2.11E+17	0.9907	0.01
Average	162.22			163.71				

0.5 to 0.7 for the KAS methods. During this process, the decomposition of most of the lignin and residual cellulose might happen. With the extent of conversion of 0.7-0.9, the corresponding activation energy also increased to 225.80 kJ/mol. The similar trend of activation energy calculated was observed from the FWO methods. The mean activation energies calculated from KAS and FWO methods were 162.22 kJ/mol and 163.71 kJ/mol, respectively. The results calculated from KAS and FWO methods were in a good agreement with a deviation below 5.0%. The agreement validated the reliability of calculations and confirmed the predictive power of KAS and FWO methods.

Generally, it was well known that the activation energy was considered to be the minimum energy barrier that needs to overcome this barrier to start the reaction [1]. It can be seen from the previous results that there was no obvious difference proving the accuracy and accordance of two kinds of kinetic models. So it determined the sensitivity and reactivity of the reaction rate. It also showed that the complexity of this physical and chemical transformation. According to the results from tab. 3, the activation energy obtained from the untreated sample was larger than that of the treated olive waste at each extent of conversion. It was suggested that ultrasound-assisted enzyme hydrolysis could be applied to the extraction of valuable compounds from olive waste, and this method also contributed to the decomposition reaction of the sample due to the changes in composition and structure.

Kinetic analysis using CR method

The kinetic parameters were obtained from the slopes and intercepts of linear plots according to the equations given in tab. 1. The activation energy calculated by CR method was presented in tab. 4. The results showed that the activation energy obtained for untreated and

treated olive waste under nitrogen increased as the heating rate increases for the same reaction mechanism model. The same phenomenon was also reported by [26]. Furthermore, the experimental data obtained from the pyrolysis process linearly fitted into the kinetic equations selected by regression analysis, and compared to other kinetic mechanism equations, the correlation coefficients of F₂ model for this pyrolysis stage of olive waste untreated and treated were high and over 99%. It was indicated that F₂ model ($f(\alpha) = (1 - \alpha)^2$) was predominant mechanism of

Table 4. Kinetic parameters obtained by applying CR method for the pyrolysis of olive waste

Sample Number	$\beta = 5 \text{ }^\circ\text{C}/\text{min}$			$\beta = 10 \text{ }^\circ\text{C}/\text{min}$			$\beta = 15 \text{ }^\circ\text{C}/\text{min}$			$\beta = 20 \text{ }^\circ\text{C}/\text{min}$		
	E_a [kJmol ⁻¹]	A [min ⁻¹]	R ²	E_a [kJmol ⁻¹]	A [min ⁻¹]	R ²	E_a [kJmol ⁻¹]	A [min ⁻¹]	R ²	E_a [kJmol ⁻¹]	A [min ⁻¹]	R ²
F ₁	30.22	15.71	0.9802	31.61	47.26	0.9794	31.83	54.72	0.9756	32.58	82.52	0.9720
F ₂	46.32	1.1E+3	0.9909	47.83	2.5E+3	0.9927	48.79	4.0E+3	0.9911	49.98	6.5E+3	0.9929
F ₃	66.37	1.7E+5	0.9649	68.27	7.2E+5	0.9687	69.92	7.0E+5	0.9681	71.66	1.2E+6	0.9730
D ₁	47.38	233.9	0.9230	48.82	807.1	0.9203	49.74	854.8	0.9166	50.72	1.3E+3	0.9092
D ₂	53.58	593.4	0.9486	55.43	2.2E+3	0.9463	56.25	2.2E+3	0.9428	57.38	3.5E+3	0.9368
D ₃	61.53	1.4E+6	0.9725	63.93	4.0E+3	0.9708	64.61	3.9E+3	0.9678	65.95	6.4E+3	0.9636
D ₄	56.19	258.3	0.9579	58.22	971.4	0.9558	59.00	980.8	0.9525	60.20	1.6E+3	0.9471
A ₂	10.24	0.1133	0.9481	10.35	0.2903	0.9495	10.91	0.3687	0.9388	11.24	0.5283	0.9317
A ₃	3.588	0.0110	0.8039	3.757	0.0283	0.8309	3.931	0.0359	0.7880	4.125	0.0513	0.7760
G ₂	23.95	1.399	0.9416	24.92	3.963	0.9403	25.24	4.732	0.9346	25.82	6.956	0.9278
G ₃	25.90	1.611	0.9576	26.01	4.646	0.9563	27.30	5.495	0.9513	27.93	8.142	0.9456
P ₂₃	33.10	13.57	0.9100	34.63	41.33	0.9077	34.80	47.15	0.9030	35.51	70.23	0.8949
F ₁	35.22	53.04	0.9831	36.25	106.17	0.9851	37.65	205.4	0.9831	37.89	266.95	0.9817
F ₂	53.40	5.5E+3	0.9947	54.95	1.1E+4	0.9960	57.01	2.4E+4	0.9969	57.42	3.1E+4	0.9973
F ₃	76.04	1.5E+6	0.9708	78.22	3.0E+6	0.9717	81.11	7.4E+6	0.9744	81.74	9.7E+6	0.9758
D ₁	54.46	1.2E+3	0.9252	56.01	2.4E+3	0.9260	57.95	5.1E+3	0.9224	58.29	6.5E+3	0.9195
D ₂	61.44	3.7E+3	0.9500	63.20	7.3E+3	0.9512	65.40	1.6E+4	0.9481	65.80	2.0E+4	0.9458
D ₃	70.41	7.6E+3	0.9736	72.44	1.6E+6	0.9750	74.96	3.6E+4	0.9726	75.44	4.6E+4	0.9710
D ₄	64.39	1.7E+3	0.9592	66.24	3.4E+3	0.9605	68.54	7.6E+3	0.9576	68.96	9.7E+3	0.9555
A ₂	12.76	0.2412	0.9616	13.15	0.4776	0.9655	13.81	0.8323	0.9626	13.89	1.088	0.9599
A ₃	5.278	0.0232	0.8890	5.452	0.0458	0.8989	5.866	0.0787	0.8973	5.885	0.1029	0.8905
G ₂	28.15	4.018	0.9471	28.97	8.007	0.9490	30.12	14.89	0.9458	30.29	19.32	0.9432
G ₃	30.36	4.861	0.9618	31.25	9.702	0.9638	32.47	18.26	0.9609	32.66	23.71	0.9588
P ₂₃	38.42	48.68	0.9145	39.52	97.20	0.9155	40.97	188.9	0.9118	41.19	243.1	0.9085

reaction kinetic model during the whole stage of degradation for two samples. According to the energy compensation effect equation, eq. (5), compensation effect coefficients, a and b , *i. e.* the slope and intercept were obtained from the corresponding equation [23]. Therefore, the energy compensation effect equations of olive waste untreated and treated were $\ln A = 0.49E_a - 15.49$ ($R^2 = 0.9913$), and $\ln A = 0.42E_a - 13.54$ ($R^2 = 0.9930$), respectively.

Thermodynamic parameters of pyrolysis for olive waste untreated and treated

The thermodynamic parameters were obtained at a specific temperature, which was the DTG peak temperature, since this temperature characterized the highest rate of the decomposition process [4]. It was noteworthy that the CR method belonged to the model-fit method which was not accurate for apparent activation energy evaluation [27]. However, KAS and FWO method was more reliable, average activation energies could be obtained from these models [28]. According to corresponding equations, ΔG , ΔH , and ΔS were determined to evaluate the thermodynamic characteristics of the main pyrolysis process. The thermodynamic parameters of thermal decomposition of olive waste have been shown in tab. 5. The changes of enthalpies revealed the energy difference between before and after decomposition. The results (196.31 kJ/mol and 157.94 kJ/mol) were similar to the activation energy obtained from the experiment. The change of Gibbs free energy illustrated the total energy increase of the pyrolysis system [4]. The values of ΔG were 156.25 kJ/mol and 155.03 kJ/mol, respectively. In addition, entropy could also reflect the arrangement degree of carbon layer in decomposed sample. As shown in tab. 5, all values of ΔS were positive, which illustrated that the structures of substance were more disorderly compared to the initial samples at a specific temperature [4, 29]. Although there were some differences in the values of the thermodynamic parameters for the untreated and treated olive waste, the thermodynamic characteristics were consistent. The enthalpy change, Gibbs free energy, and entropy change were positive, in accordance with the results of previous literature [4].

Table 5. Thermodynamic parameters of the main pyrolysis process for the olive waste

Sample	E_a [kJmol ⁻¹]	A [min ⁻¹]	ΔH [kJmol ⁻¹]	ΔG [kJmol ⁻¹]	ΔS [Jmol ⁻¹]
Raw olive waste	201.41	8.92E+16	196.31	156.25	65.27
Treated olive waste	162.97	6.11E+13	157.94	155.03	4.805

Conclusions

The pyrolysis of raw and ultrasound-enzyme hydrolysis treated olive waste had been investigated under nitrogen atmosphere at different heating rates by the means of TG analysis. The degradation process divided into three stages and the heating rate has a significant impact on weight loss at each stage. The weight loss is dramatically increased in the second zone, which may be caused by the decomposition of the hemicellulose, cellulose and lignin at the temperature ranges. As the heating rates increased, the temperature interval and peak temperature moved toward higher temperature. The DTG and DSC curves showed that the treated olive waste changed in composition and structure compared to the untreated sample. The KAS and FWO methods exhibited the similar kinetic parameters during the TG analysis, and the activation energy of untreated olive waste was significantly higher than that of the treated sample. Meanwhile, the activation energy was closely related to the extent of conversion. The CR method suggested the second-order model [$f(\alpha) = (1 - \alpha)^2$] might be used to describe the thermal

decomposition mechanism of olive waste untreated and treated. Besides, thermodynamic characteristics of raw and treated olive waste were consistent.

Acknowledgment

The authors acknowledge funding support from the National Key Research and Development Program of China (NO. 2017YFF0207804), the GDAS' Special Project of Science and Technology Development (NO. 2017GDASCX-0702) and the National Natural Science Foundation of China (NO. 31660181).

Nomenclature

A	– pre-exponential factor, [min^{-1}]	K_B	– Boltzmann constant
E	– activation energy of the reaction, [Jmol^{-1}]	R	– ideal gas constant, [$8.314 \text{ Jmol}^{-1}\text{K}^{-1}$]
$f(\alpha)$	– function depending on the decomposition mechanism	ΔS	– change values of entropy, [Jmol^{-1}]
ΔG	– change values of Gibbs free energy, [kJmol^{-1}]	T	– absolute temperature, [K]
$g(\alpha)$	– integral form of $f(\alpha)$	T_{max}	– peak temperature of DTG, [K]
ΔH	– change values of enthalpy, [kJmol^{-1}]	<i>Greek symbols</i>	
h	– Plank constant	α	– extent of conversion
		β	– heating rate, [$^{\circ}\text{Cmin}^{-1}$]

References

- [1] Huang, X., *et al.*, Pyrolysis Kinetics of Soybean Straw Using Thermogravimetric Analysis, *Fuel*, 169 (2016), 7, pp. 93-98
- [2] Jauhiainen, J., *et al.*, Kinetics of the Pyrolysis and Combustion of Olive Oil Solid Waste, *Journal of Analytical and Applied Pyrolysis*, 72 (2004), 1, pp. 9-15
- [3] Putun, A. E., *et al.*, Bio-Oil from Olive Oil Industry Wastes: Pyrolysis of Olive Residue under Different Conditions, *Fuel Processing Technology*, 87 (2005), 1, pp. 25-32
- [4] Islam, M. A., *et al.*, Pyrolysis Kinetics of Raw and Hydrothermally Carbonized Karanj (Pongamia Pinnata) Fruit Hulls Via Thermogravimetric Analysis, *Bioresource Technology*, 179 (2015), 5, pp. 227-233
- [5] Islam, M. A., *et al.*, Combustion Kinetics of Hydrochar Produced from Hydrothermal Carbonization of Karanj (Pongamia Pinnata) Fruit Hulls Via Thermogravimetric Analysis, *Bioresource Technology*, 194 (2015), 20, pp. 14-20
- [6] Shin, S., *et al.*, Kinetic Analysis Using Thermogravimetric Analysis for Nonisothermal Pyrolysis of Vacuum Residue, *Journal of Thermal Analysis and Calorimetry*, 126 (2016), 2, pp. 933-941
- [7] Buratti, C., *et al.*, Thermogravimetric Analysis of the Behavior of Sub-Bituminous Coal and Cellulosic Ethanol Residue During Co-Combustion, *Bioresource Technology*, 186 (2015), 12, pp. 154-162
- [8] Bartocci, P., *et al.*, Pyrolysis of Pellets Made with Biomass and Glycerol: Kinetic Analysis and Evolved Gas Analysis, *Biomass and Bioenergy*, 97 (2017), 2, pp. 11-19
- [9] Xu, Y. L., *et al.*, Investigation of Thermodynamic Parameters in the Pyrolysis Conversion of Biomass and Manure to Biochars Using Thermogravimetric Analysis, *Bioresource Technology*, 146 (2013), 20, pp. 485-493
- [10] Sebio-Punal, T., *et al.*, Thermogravimetric Analysis of Wood, Holocellulose, and Lignin from Five Wood Species, *Journal of Thermal Analysis and Calorimetry*, 109 (2012), 3, pp. 1163-1167
- [11] Araujo, M., *et al.*, Phenolic Compounds from Olive Mill Wastes: Health Effects, Analytical Approach and Application as Food Antioxidants, *Trends in Food Science and Technology*, 45 (2015), 2, pp. 200-211
- [12] Garcia-Ibanez, P., *et al.*, Thermogravimetric Analysis of Olive-Oil Residue in Air Atmosphere, *Fuel Processing Technology*, 87 (2006), 2, pp. 103-107
- [13] Ounas, A., *et al.*, Pyrolysis of Olive Residue and Sugar Cane Bagasse: Non-Isothermal Thermogravimetric Kinetic Analysis, *Bioresource Technology*, 102 (2011), 24, pp. 11234-11238
- [14] Ozveren, U., *et al.*, Investigation of the Slow Pyrolysis Kinetics of Olive Oil Pomace Using Thermo-Gravimetric Analysis Coupled with Mass Spectrometry, *Biomass & Bioenergy*, 58 (2013), 11, pp. 168-179
- [15] Rubio-Senent, F., *et al.*, Isolation and Identification of Minor Secoiridoids and Phenolic Components from Thermally Treated Olive Oil by-Products, *Food Chemistry*, 187 (2015), 22, pp. 166-173

- [16] Wang, Z. H., *et al.*, Ultrasound-Assisted Enzyme Catalyzed Hydrolysis of Olive Waste and Recovery of Antioxidant Phenolic Compounds, *Innovative Food Science and Emerging Technologies*, 44 (2017), 6, pp. 224-234
- [17] Yahiaoui, M., *et al.*, Determination of Kinetic Parameters of Phlomis Bovei De Noé Using Thermogravimetric Analysis, *Bioresource Technology*, 196 (2015), 22, pp. 441-447
- [18] Kissinger, H. E. Reaction Kinetics in Differential Thermal Analysis, *Analytical Chemistry*, 29 (1957), 11, pp. 1702-1706
- [19] Garcia-Maraver, A., *et al.*, Determination and Comparison of Combustion Kinetics Parameters of Agricultural Biomass from Olive Trees, *Renewable Energy*, 83 (2015), 11, pp. 897-904
- [20] Flynn, J. H., *et al.*, A Quick, Direct Method for the Determination of Activation Energy from Thermogravimetric Data, *Journal of Polymer Science Part B: Polymer Letters*, 4 (1996), 5, pp. 323-328
- [21] Ozawa, T. A New Method of Analyzing Thermogravimetric Data, *Bulletin of the Chemical Society of Japan*, 38 (1965), 11, pp. 1881-1886
- [22] Coats, A. W., *et al.*, Kinetic Parameters from Thermogravimetric Data, *Nature*, 201 (1964), 68, pp. 68-69
- [23] Hu, Z. Q., *et al.*, Characteristics and Kinetic Studies of Hydrilla Verticillata Pyrolysis Via Thermogravimetric Analysis, *Bioresource Technology*, 194 (2015), 20, pp. 364-372
- [24] Lesnikovich, A. I., *et al.*, A Method of Finding Invariant Values of Kinetic, *Journal of Thermal Analysis*, 27 (1983), 1, pp. 89-94
- [25] Rahman, Md. R., *et al.*, Differential Scanning Calorimetry (DSC) and Thermogravimetric Analysis (TGA) of Wood Polymer Nanocomposites, *MATEC Web of Conference*, 87 (2017), Aug., pp. 03013
- [26] Shen, D. K., *et al.*, Kinetic Study on Thermal Decomposition of Woods in Oxidative Environment, *Fuel*, 88 (2009), 6, pp. 1024-1030
- [27] Hu, M., *et al.*, Thermogravimetric Study on Pyrolysis Kinetics of Chlorella Pyrenoidosa and Bloom-Forming Cyanobacteria, *Bioresource Technology*, 177 (2015), 3, pp. 41-50
- [28] Ceylan, S., *et al.*, Pyrolysis Kinetics of Hazelnut Husk Using Thermogravimetric Analysis, *Bioresource Technology*, 156 (2014), 9, pp. 182-188
- [29] Ruvolo-Filho, A., *et al.*, Chemical Kinetic Model and Thermodynamic Compensation Effect of Alkaline Hydrolysis of Waste Poly (Ethylene Terephthalate) in Nonaqueous Ethylene Glycol Solution, *Industrial and Engineering Chemistry Research*, 45 (2006), 24, pp. 7985-7996